Experimental Observation and Theoretical Description of Multisoliton Fission in Shallow Water

S. Trillo,[1,*] G. Deng,[2] G. Biondini,[2,3] M. Klein,[4] G. F. Clauss,[4] A. Chabchoub,[5,6] and M. Onorato[7,8,†]
[1]Dipartimento di Ingegneria, Università di Ferrara, Via Saragat 1, 44122 Ferrara, Italy
[2]State University of New York at Buffalo, Department of Physics, Buffalo, New York 14260-2900, USA
[3]State University of New York at Buffalo, Department of Mathematics, Buffalo, New York 14260-2900, USA
[4]Ocean Engineering Division, Technical University of Berlin, Salzufer 17-19, 10587 Berlin, Germany
[5]Department of Mechanical Engineering, Aalto University, 02150 Espoo, Finland
[6]Department of Ocean Technology Policy and Environment, Graduate School of Frontier Sciences, The University of Tokyo, Kashiwa, Chiba 277-8563, Japan
[7]Dipartimento di Fisica, Università di Torino, Via P. Giuria, 1, 10125 Torino, Italy
[8]Istituto Nazionale di Fisica Nucleare, Sezione di Torino, Via P. Giuria, 1, 10125 Torino, Italy
(Received 22 April 2016; published 28 September 2016)

We observe the dispersive breaking of cosine-type long waves [Phys. Rev. Lett. **15**, 240 (1965)] in shallow water, characterizing the highly nonlinear "multisoliton" fission over variable conditions. We provide new insight into the interpretation of the results by analyzing the data in terms of the periodic inverse scattering transform for the Korteweg–de Vries equation. In a wide range of dispersion and nonlinearity, the data compare favorably with our analytical estimate, based on a rigorous WKB approach, of the number of emerging solitons. We are also able to observe experimentally the universal Fermi-Pasta-Ulam recurrence in the regime of moderately weak dispersion.

DOI: 10.1103/PhysRevLett.117.144102

Introduction.—In a Letter that gave birth to modern soliton science [1], Zabusky and Kruskal (ZK) showed that cosine waves propagating according to the weakly dispersing Korteweg–de Vries (KdV) equation [2] undergo a gradient catastrophe that generates "solitons." Their interaction leads to recursive behavior, thus confirming, in the continuum limit, the phenomenon discovered by Fermi-Pasta-Ulam (FPU) for oscillator chains [3].

Recently, problems involving the dispersive breaking of waves have attracted renewed interest, thanks to experiments in nonlinear optics, Bose Einstein condensation, electron beams, and spin waves, which reported the catastrophe-induced generation of solitons [4–6], dispersive shock waves [7,8], and different regimes of FPU recurrence [9,10]. Specific experiments for the *periodic* case were reported just recently by exploiting an optical harmonic (or modulated) wave ruled by the nonlinear Schrödinger model [11]. Conversely, for the KdV equation, little progress has been made since the early experiments on breaking of periodic waves in electrical transmission lines, water, and ion acoustic waves [12–15]. In particular, in experiments on surface gravity waves described by the KdV [16], the recurrence phenomenon predicted by ZK remained elusive, and the observation of fission was limited to a few solitons [13,17,18], which left open even basic questions such as how many solitons can be expected to emerge under variable experimental conditions. Furthermore, a comprehensive interpretation of experimental data on the fission process in terms of inverse scattering transform (IST, also known as nonlinear Fourier transform) [17,19,20], and, in particular, the finite-gap theory valid for the periodic case [21–24] is still lacking, also due to the intrinsic difficulty to obtain analytical predictions.

In this Letter we present an extensive experimental investigation performed in a long tank, which provides both evidence for recurrence and, at different water depths and wave amplitudes, a quantitative validity test of the KdV description of the multisoliton fission. We also present a theoretical description combining IST and the Wentzel-Kramers-Brillouin (WKB) method which provides an analytical characterization of the experiment in terms of a formula that yields the number of solitonlike excitations as a function of a single overall dimensionless parameter quantifying the relative smallness of dispersive effects.

Experiment.—The experiment was performed in the sea-keeping basin of the Technical University of Berlin, which is $8\ \mathrm{m} \times 110\ \mathrm{m}$, with an effective measuring range of 90 m. On one side, a computer assisted wave generator is installed, which, in the present experiment, was utilized in a piston-type mode. It provides a horizontal particle velocity profile at the wave board close to the physical one. The hydrodynamic transfer function of the wave generator is modeled using the Biesel function [25], relating the wave board stroke to the wave amplitude at the position of the wave maker linearly. On the opposite (downstream) side, a wave damping slope is installed to limit wave reflections. The setup comprises eight equally spaced wave gauges that are installed along the basin at distances $z_j = 5 + (j-1)10$ m, $j = 1, 2, \ldots, 8$, from the wave maker located at $z = 0$. The computer controlled wave maker produced,

after a short ramp, a burst of eight periods of a harmonic wave with adjustable elevation η_0 and period $T = 2\pi/\omega$. We measured the elevation of the propagating wave train as time series $\eta(t, z_j)$ at gauge locations z_j. Consistently, the theoretical framework is based on the following initial value problem, involving the KdV equation, written as a dimensional evolution equation in space [26]

$$\eta_z + \frac{1}{c_0}\eta_t - \alpha\eta\eta_t - \beta\eta_{ttt} = 0; \quad \eta(t,0) = \eta_0\cos(\omega t), \qquad (1)$$

where $c_0 = \sqrt{gh}$ is the linear (nondispersive) velocity in shallow water of rest level h, $\alpha = \frac{3}{2}(1/c_0 h)$, and $\beta = \frac{1}{6}(h^2/c_0^3)$. The evolution dynamics is ruled by the interplay of two characteristic length scales associated with the temporal duration t_0, namely, the nonlinear length $L_{\rm nl} = (t_0/\alpha\eta_0)$ and the dispersion length $L_d = (t_0^3/\beta)$ (see also Ref. [27]). Without loss of generality, we set $t_0 = (T/2\pi) = (1/\omega)$, which amounts to choosing $L_{\rm nl}$ exactly equal to the breaking distance $L_b = 1/\max[(d/dt)\alpha\eta(t,0)] = 1/(\alpha\omega\eta_0)$, after which the cosine wave would develop the gradient catastrophe in the dispersionless limit $\beta = 0$. While $L_{\rm nl}$ determines the physical length scale for the critical steepening and the ensuing fission, the number of solitons that emerge from the process is determined only by the value of the dimensionless parameter $\varepsilon^2 = 6L_{\rm nl}/L_d = 2\omega^2 h^3/(3\eta_0 c_0^2)$, which measures the smallness of dispersion, and is inversely proportional to the Ursell number [27,28]. This can be seen by casting Eqs. (1) in dimensionless units as

$$u_\zeta - 6uu_\tau - \varepsilon^2 u_{\tau\tau\tau} = 0; \qquad u_0(\tau) = \cos(\tau), \qquad (2)$$

where $u(\zeta,\tau) = \eta/\eta_0$, $\tau = \omega(t - z/c_0)$ is the normalized retarded time, $\zeta = z/(6L_{\rm nl})$, and ε is the only parameter left. The value of ε is linked to that of the parameter δ used by ZK as $\varepsilon^2 = 6\pi^2\delta^2$ [1].

In the experiment, we measured the evolution of the waves at different depths $h = 10$, 15, 20, 26, 40 cm and wave amplitudes η_0, which we always kept below the threshold $\eta_0^{\rm th}$ for the onset of turbulent breaking (note that $\eta_0^{\rm th}$ decreases proportionally to h). Typical values of the parameters for five different runs at different depths are reported in Table I. The regime of run A [29], in which $\varepsilon^2 \simeq 0.07$ is relatively large, essentially corresponds to the regime of early experiments characterized by very few emerging solitons (≤ 4 in Ref. [13]). However, by decreasing the water depth h, one can obtain both a shorter nonlinear length $L_{\rm nl}$ and a smaller dispersion parameter ε; this follows from the fact that $L_{\rm nl} \sim h^{3/2}$, $L_d \sim h^{-1/2}$, and hence $\varepsilon^2 \sim h^2$. In particular, as shown in Table I, at $h = 20$ and $\eta_0 = 1.84$ cm, run B corresponds to $\varepsilon^2 \simeq 0.029$, which is almost identical to the value $\delta = 0.022$ considered by ZK [1]. The full measured evolution of this case is displayed in Fig. 1. Steepening occurs in time over the positive slope

TABLE I. Experimental parameters for five representative runs: water depth h, initial amplitude η_0, period T, dispersion length L_d, nonlinear length $L_{\rm nl}$, and dispersion smallness ε^2 [related to δ^2 used by ZK as $\delta^2 = \varepsilon^2/(6\pi^2)$]. See Fig. 1 for run B, Fig. 2 for runs C–D, Fig. 5 for run E.

	run A	run B	run C	run D	run E (recur.)
η_0 [cm]	3.11	1.84	1.70	1.24	5.50
h [m]	0.4	0.2	0.15	0.1	0.4
T [s]	14.0	14.1	14.0	14.1	5.0
L_d [m]	3252	4713	5266	6651	147
$L_{\rm nl}$ [m]	37.95	22.86	15.90	11.99	7.64
ε^2	0.0701	0.0290	0.0181	0.0107	0.3122

front of the cosine until tiny ripples appear to regularize the strong gradient observed at $z_3 = 25$ m, which is close to the breaking distance $z = L_{\rm nl} \simeq 23$ m for the dispersionless limit $\varepsilon = 0$. Such oscillations expand and become deeper, forming undular bores at $z_{4,5} = 35$, 45 m, until they eventually lead, at $z_{6,7} = 55$, 65 m, to the formation of solitonlike excitations on a finite negative background, whose peaks scale approximately linearly. The peak amplitudes agree well with the predictions based on the IST analysis of data (see below) and reported as open dots in Figs. 1(f), 1(g). As shown by the data recorded at the last gauge, the fission proceeds until up to eight solitonlike excitations on the same background appear at $z_8 = 75$ m,

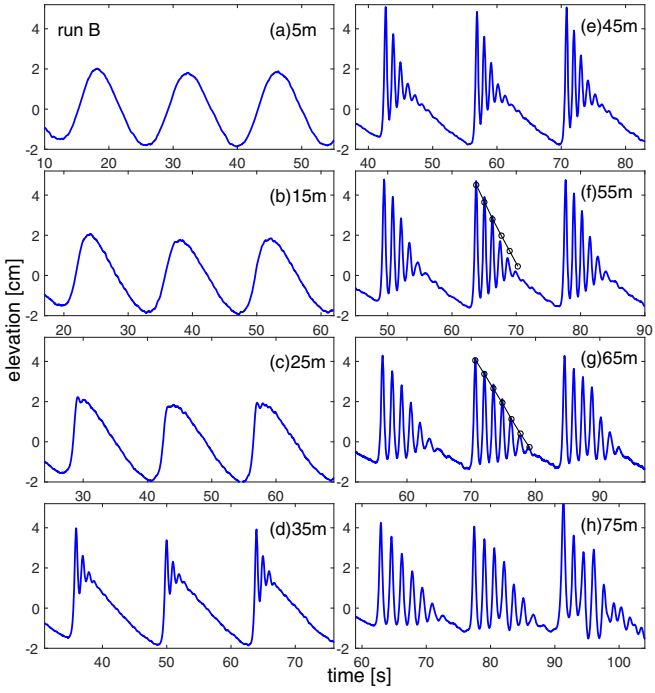

FIG. 1. Fission from three periods of a cosine wave with $\eta_0 = 1.84$ cm in $h = 20$ cm water (run B in Table I). In order to follow the evolution of the same initial period, different time intervals are displayed. Open dots in (f), (g) stand for soliton amplitudes computed from IST analysis of data sets [see text and Fig. 3(b)], recorded at 55 and 65 m.

as shown in Fig. 1(h). Note that, at this stage, the regularity of the periods becomes affected by the residual reflection of the forefront periods arrived at the tank end.

When we further decrease the water depth to $h = 15$ cm (run C in Table I) and $h = 10$ cm (run D in Table I), the steepening is found to occur on a shorter length scale according to the reduced values of $L_{\rm nl}$ (see Table I). In fact, as shown in Figs. 2(a) and 2(d), well developed oscillations already appear at $z_3 = 25$ m. In this case, the fission gives rise to a maximum of 10 (at distance $z_7 = 65$ m) and 12 (at $z_6 = 55$ m) distinguishable solitons in the case of run C and run D, respectively. However, as ε^2 decreases and the number of solitons increases, counting them by visual inspection of the time series becomes inappropriate for two basic reasons: (i) fission of solitons can proceed until the wave train exceeds one period of the cosine wave, a condition where shallow solitons can be easily hidden by the tall ones in the adjacent period; (ii) the waves produced through the dispersive breaking are not, strictly speaking, soliton solutions, but rather finite-gap solutions, and not all the bands correspond to visible excitations with solitonlike features. Therefore a criterion is needed to define the latter.

IST data analysis.—Both of the issues mentioned above can be successfully addressed by analyzing the experimental data in terms of the IST for periodic potentials (p-IST) [17,19,20]. Explicitly, the nonlinear wave components contained in the input monochromatic wave $u_0(\tau) = \cos(\tau)$ can be computed via the direct scattering eigenvalue problem associated to Eq. (2), namely, the time-independent Schrödinger equation

$$\varepsilon^2 \phi_{\tau\tau} + (\lambda + u)\phi = 0, \tag{3}$$

λ being the spectral parameter. When $u = u_0(\tau)$, Eq. (3) is the Mathieu equation. Floquet (Bloch) theory implies that

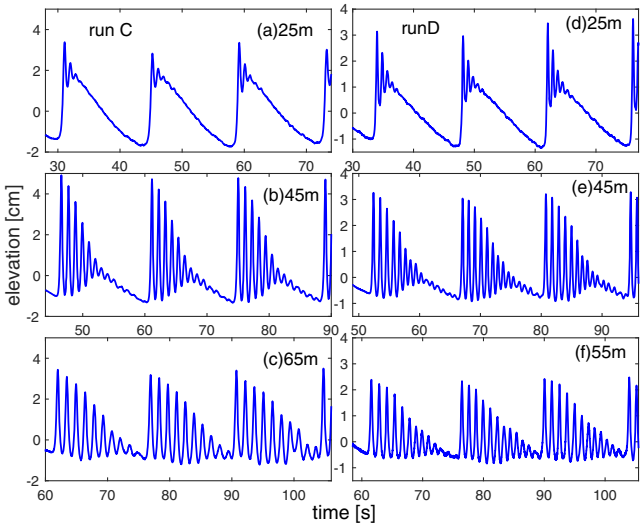

FIG. 2. Wave profiles: (a)–(c) run C, $h = 15$ cm, $\varepsilon^2 = 0.0181$; (d)–(f) run D, $h = 10$ cm, $\varepsilon^2 = 0.0107$.

the spectrum of Eq. (3) decomposes into alternating bands and gaps, with the former corresponding to the waves that are embedded in the initial condition and progressively emerge from the fission. Of particular importance here is the main spectrum, which is invariant upon evolution, and is constituted by the band edges λ_{2n-1} and λ_{2n}, $n = 1, \ldots, N$, where N is the number of gaps. Such values are defined by the conditions $T(\lambda_{2n-1}) = 1$ and $T(\lambda_{2n}) = -1$ for n odd ($1 \leftrightarrow -1$ for n even), where $T(\lambda) = \frac{1}{2}\mathrm{Trace}(M)$ and M is the monodromy matrix associated with Eq. (3) [17,19,20,22]. The corresponding spectral bands are $[\lambda_{2n-1}, \lambda_{2n}]$, $n = 1, \ldots, N$, plus $[\lambda_{2N+1}, \infty)$, for which $|T(\lambda)| \leq 1$. Solitons are obtained in the limit where the bandwidths shrink to zero; i.e., the band edges coincide, $\lambda_{2n-1} = \lambda_{2n}$. This condition is never strictly satisfied in the periodic case. Nevertheless, one can say that the nth band yields an effective soliton if the relative bandwidth $W_n = w_n/(w_n + g_n)$ is sufficiently small, $w_n = \lambda_{2n} - \lambda_{2n-1}$ and $g_n = \lambda_{2n+1} - \lambda_{2n}$ being, respectively, the bandwidth and the adjacent gap width. A suitable choice is $W_n \leq \kappa$, with $\kappa = 0.01$ [31]. Under these conditions the soliton amplitudes can be calculated as $A_n = 2(\lambda_{\rm ref} - \lambda_{2n})$, $n = 1, \ldots, N_s$, where $\lambda_{\rm ref} = \lambda_{2N_s+1}$ stands for the reference level [29], and $N_s < N$ is the number of solitons (bands fulfilling $W_n \leq \kappa$) [22,32].

To determine the number of solitons N_s in the experiment, we compared the p-IST spectrum for a cosine wave $u_0(\tau) = \cos\tau$ with the spectrum of the measured data. That is, for the latter we replaced u in Eq. (3) with the normalized recorded data $u_j(\tau) = \eta(\omega t, z_j)/\eta_0$, which amounts to measuring the amplitude in units of η_0 and to normalizing the period to 2π. The results of such analysis are shown in Fig. 3 for run B, corresponding to the ZK regime. In particular, Fig. 3(a) compares the half-trace $T(\lambda)$ for the pure cosine input and the data measured at distance $z_6 = 55$ m, displaying very good agreement between the two. Of the ten total bands, only the first eight fulfill the criterion $W_n \leq \kappa$ (those on the left of the threshold λ_s), giving rise to 8 solitonlike excitations in agreement with the visual count from Fig. 1. We repeated this analysis at distances z_j, $j = 1, \ldots, 7$ (gauge 8 was excluded due to the presence of reflection). The dimensional soliton amplitudes $\eta_0 A_n = 2\eta_0(\lambda_{\rm ref} - \lambda_{2n})$, obtained from the calculated band edges at $z = z_j$, are plotted in Fig. 3(b) as a function of distance, which shows a good degree of constancy, confirming the spectrum invariance upon evolution.

We performed the above analysis for all recorded data sets, obtaining N_s as a function of ε. The p-IST results were obtained by numerically integrating Eq. (3), as in Refs. [22,32]. In the case of the pure cosine input, however, we can also obtain all spectral information analytically by employing the WKB expansion $\phi(x) = A(x)e^{iS(x)/\varepsilon}$ in the Mathieu equation. Leaving all the mathematical details to a separate publication for brevity [33], this approach allows us to obtain analytical

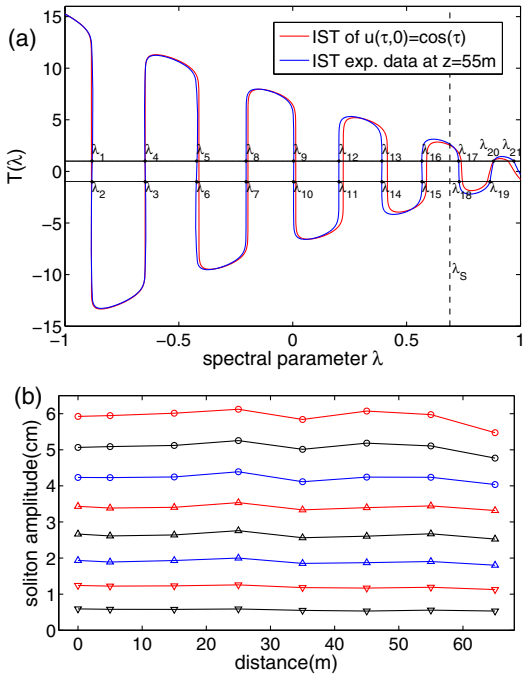

FIG. 3. (a) Half-trace of monodromy matrix $T(\lambda)$ vs spectral parameter λ at $\varepsilon^2 = 0.029$ (ZK regime), comparing the ideal monochromatic case $u_0 = \cos(\tau)$, with normalized experimental data, run B, $z_6 = 55$ m [Fig. 1(f)]. $\lambda_{1,\ldots,21}$ are the band edges; $N_s = 8$ solitons correspond to the first eight bands on the left of λ_S (see text for its definition). This sets $\lambda_{\rm ref}$ to λ_{17} ($2N_s + 1 = 17$). (b) Real-world soliton amplitudes $2\eta_0[\lambda_{17}(z_j) - \lambda_{2n}(z_j)]$, $n = 1, \ldots, 8$, obtained from the p-IST analysis, as reported in (a), of recorded elevation $\eta(t, z_j)$ at gauge distances z_j [data at $z = 0$, obtained from $u_0 = \cos(\tau)$, are reported for reference].

expressions for the monodromy matrix M and the relative bandwidths W_n, from which we estimate N_s as

$$N_s = \left\lfloor \frac{2S_1(\lambda_s)}{\pi\varepsilon} + \frac{1}{2} \right\rfloor, \tag{4}$$

$\lfloor\cdot\rfloor$ being the floor function, $S_1(\lambda) = 2\sqrt{1+\lambda}E(\varphi, k)$ and $E(\cdot)$ the incomplete elliptical integral of second kind with argument $\varphi = [\pi - \cos^{-1}(\lambda)]/2$ and modulus $k = \sqrt{2/(1+\lambda)}$. The value λ_s, which as before is the threshold at which $W_n = \kappa$ [cf. Fig. 3(a)], can now be obtained as $S_2(\lambda_s) = \varepsilon \ln(2/\pi\kappa)$, with $S_2(\lambda) = 4\sqrt{1-\lambda}E(\varphi, k)$ with $\varphi = \cos^{-1}(\lambda)/2$ and $k = \sqrt{2/(1-\lambda)}$. The comparison between the estimate in Eq. (4) and the number of solitons obtained from all available data sets (by applying the p-IST numerical analysis illustrated in Fig. 3) is displayed in Fig. 4, which shows a very good agreement even at relatively large values of ε, where the WKB is expected to be less accurate. Some discrepancy is observed in the most nonlinear runs at $h = 10$ cm, where, however, the effect of losses and the nonuniformity of the bottom become non-negligible. We also remark that a suitable expansion of Eq. (4) [34] shows that N_s scales at leading

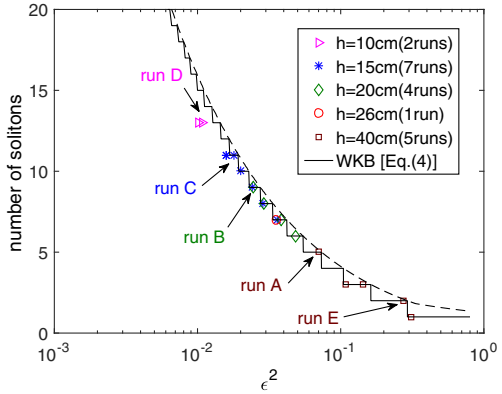

FIG. 4. Number of solitons N_s vs dispersion smallness $\varepsilon^2 = (2\omega^2 h^2/3g\eta_0)$, as extracted from p-IST of experimental data at $z_6 = 55$ m. Equal symbols and colors indicate data sets recorded at same depth h. The solid line stands for the WKB result in Eq. (4), $\kappa = 0.01$, with its envelope (dashed line) emphasizing leading order dependence $N_s \sim 1/\varepsilon$.

order as $1/\varepsilon \sim \sqrt{\eta_0}/\omega h$, in agreement with heuristic estimates given in the past [15,35]. Similar expansions also yield explicit estimates for the soliton amplitudes, which confirm the nearly linear variation of soliton peaks as observed in Figs. 1 and 2 and pointed out by ZK [1].

Recurrence.—In the ZK regime (run B), recurrence is expected at $z \simeq 690$ m ($\zeta \simeq 5.067$), clearly beyond most tank facilities. However, recurrence can be experimentally observed with shorter L_{nl} but larger ratio L_{nl}/L_d, as obtained, e.g., in run E in Table I. In this case, fission gives rise to three clearly visible nonlinear waves, as shown in Fig. 5. The recurrence is clearly recognized from the evolution of the amplitudes of the first three Fourier modes [see Fig. 5(a)], obtained from the recorded data [3]. Similarly to what happens in FPU (compare with Fig. 1 in Ref. [3]), the second mode attains maximum energy when the fundamental one is most depleted, then the

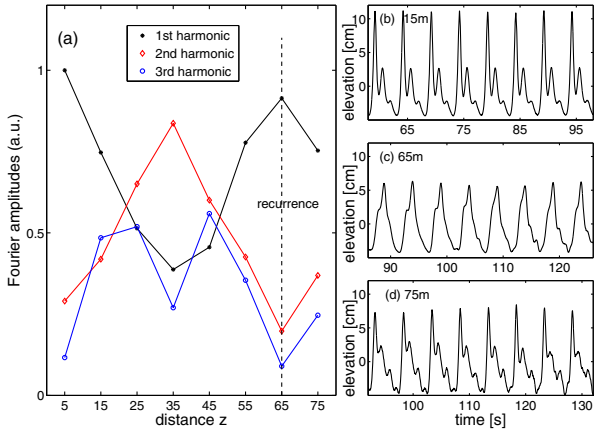

FIG. 5. Recurrence observed for run E, $h = 40$ cm: (a) Fourier mode evolution from data measured at the eight gauge locations z_j; (b)–(d) Wave profiles at $z_2 = 15$, $z_7 = 65$ (recurrence), $z_8 = 75$ m (new cycle of fission).

process is reversed until the fundamental mode takes back his energy $z_7 = 65$ m. Meanwhile, the third mode is characterized by a double cycle of amplification and deamplification. At 65 m we observe a good recurrence of the initial condition, followed by a new cycle of fission starting at 75 m.

Conclusions.—We presented extended observations of multisoliton fission and recurrence in surface gravity waves which show good agreement with novel analytical predictions on the number of emerging solitons, based on a WKB reduction of the scattering problem associated with the KdV equation. These results will be crucial to understand more complex phenomena such as wave runup [36] and coastal evolution of tsunamis [37], and, given the universality of the dispersive breaking of waves, constitute a viable general approach to understand experiments ruled by other integrable models.

We acknowledge valuable discussions with A. R. Osborne. S. T. and M. O. acknowledge support from the Italian Ministry of University and Research (MIUR) (PRIN-2012BFNWZ2). G. D. acknowledges the Department of Physics, University of Turin, for the support during her staying in Turin. G. B. acknowledges the National Science Foundation under Grants No. DMS-1311847 and No. DMS-1614623. A. C. acknowledges support from the Japan Society for the Promotion of Science (JSPS) and the Burgundy Region (PARI Photcom). M. O. also acknowledges F. Gatto for discussions during the early stages of this work.

*stefano.trillo@unife.it
†miguel.onorato@gmail.com

[1] N. J. Zabusky and M. D. Kruskal, Phys. Rev. Lett. **15**, 240 (1965).
[2] J. Korteweg and G. De Vries, Philos. Mag. **39**, 422 (1895).
[3] E. Fermi, J. Pasta, and S. Ulam, in *Collected Papers of Enrico Fermi*, edited by E. Segré (The University of Chicago, Chicago, 1965), Vol. 2, pp. 977 (Fig. 1 at page 982).
[4] Z. Dutton, M. Budde, C. Slowe, and L. V. Hau, Science **293**, 663 (2001).
[5] C. Conti, A. Fratalocchi, M. Peccianti, G. Ruocco, and S. Trillo, Phys. Rev. Lett. **102**, 083902 (2009).
[6] Y. C. Mo, R. A. Kishek, D. Feldman, I. Haber, B. Beaudoin, P. G. O'Shea, and J. C. T. Thangaraj, Phys. Rev. Lett. **110**, 084802 (2013).
[7] M. A. Hoefer, M. J. Ablowitz, I. Coddington, E. A. Cornell, P. Engels, and V. Schweikhard, Phys. Rev. A **74**, 023623 (2006).
[8] W. Wan, S. Jia, and J. W. Fleischer, Nat. Phys. **3**, 46 (2007); N. Ghofraniha, C. Conti, G. Ruocco, and S. Trillo, Phys. Rev. Lett. **99**, 043903 (2007).
[9] G. Van Simaeys, Ph. Emplit, and M. Haelterman, Phys. Rev. Lett. **87**, 033902 (2001); A. Mussot, A. Kudlinski, M. Droques, P. Szriftgiser, and N. Akhmediev, Phys. Rev. X **4**, 011054 (2014).
[10] M. Wu and C. E. Patton, Phys. Rev. Lett. **98**, 047202 (2007).
[11] J. Fatome, C. Finot, G. Millot, A. Armaroli, and S. Trillo, Phys. Rev. X **4**, 021022 (2014).
[12] R. Hirota and K. Suzuki, J. Phys. Soc. Jpn. **28**, 1366 (1970).
[13] N. J. Zabusky and C. J. Galvin, J. Fluid Mech. **47**, 811 (1971).
[14] F. D. Tappert and C. N. Judice, Phys. Rev. Lett. **29**, 1308 (1972).
[15] H. Ikezi, Phys. Fluids **16**, 1668 (1973).
[16] J. L. Hammack and H. Segur, J. Fluid Mech. **65**, 289 (1974); for a review, see D. Arcas and H. Segur, Phil. Trans. R. Soc. A **370**, 1505 (2012).
[17] A. R. Osborne, *Nonlinear Ocean Waves and the Inverse Scattering Transform* (Academic Press, New York, 2010).
[18] M. Brühl and H. Oumeraci, Proceedings of the ASME 2014, 33rd International Conference on Ocean, Offshore and Arctic Engineering (OMAE2014) (Ocean Engineering, San Francisco, 2014), Vol. **8B**, Paper No. OMAE2014-24165; see also Chap. 6 in M. Brühl, PhD thesis.
[19] M. J. Ablowitz and H. Segur, *Solitons and the Inverse Scattering Transform* (SIAM, Philadelphia, 1981).
[20] S. P. Novikov, S. V. Manakov, L. P. Pitaevskii, and V. E. Zakharov, *Theory of Solitons: The Inverse Scattering Method* (Plenum, New York, 1984).
[21] B. A. Dubrovin and S. P. Novikov, Zh. Eksp. Thor. Fix. **67**, 2131 (1974) [, Sov. Phys. JETP **40**, 1058 (1975)].
[22] A. R. Osborne and L. Bergamasco, Physica (Amsterdam) **18D**, 26 (1986).
[23] S. Venakides, Trans. Am. Math. Soc. **301**, 189 (1987).
[24] A. R. Osborne, E. Segre, G. Boffetta, and L. Cavaleri, Phys. Rev. Lett. **67**, 592 (1991).
[25] F. Biésel and F. Suquet, La Houille blanche **2**, 147 (1951).
[26] A. R. Osborne and M. Petti, Phys. Rev. E **47**, 1035 (1993); Phys. Fluids **6**, 1727 (1994).
[27] S. Trillo, M. Klein, G. Clauss, and M. Onorato, Physica (Amsterdam) **333D**, 276 (2016).
[28] F. Ursell, *Proc. Camb. Phil. Soc.* 49, 685 (Cambridge University Press, Cambridge, England, 1953).
[29] See Supplemental Material at http://link.aps.org/supplemental/10.1103/PhysRevLett.117.144102 for further details on the reference level and on IST implementation, which also include Ref. [30], as well as additional recorded data.
[30] E. Falcon, C. Laroche, and S. Fauve, Phys. Rev. Lett. **89**, 204501 (2002).
[31] Incidentally, this is equivalent to a soliton index m_n, used in Refs. [22,32], $m_n \geq 1 - \kappa$, i.e., which in turn means, for the particular case of a single cn-oidal wave, that the modulus of the Jacobian function $m \geq 0.99$, to be compared with $m = 1$ for a strict soliton.
[32] I. C. Christov, Math. Comput. Simul. **82**, 1069 (2012); A. Salupere, G. A. Maugin, J. Engelbrecht, and J. Kalda, Wave Motion **23**, 49 (1996).
[33] G. Deng, G. Biondini, and S. Trillo, Physica (Amsterdam) **333D**, 137 (2016).
[34] Such an estimate can be obtained by expanding $S_1(\lambda)$ and $S_2(\lambda)$ in Taylor series around $\lambda = -1$ and $\lambda = 1$, respectively.
[35] N. J. Zabusky, J. Comput. Phys. **43**, 195 (1981).
[36] C. Viotti, F. Carbone, and F. Dias, J. Fluid Mech. **748**, 768 (2014).
[37] A. Kundu, *Tsunami and Nonlinear Waves* (Springer, Berlin, 2007).